PHYSICAL REVIEW B VOLUME 38, NUMBER 9 15 SEPTEMBER 1988-II

Microscopic structure of the SiO_2/Si interface

F. J. Himpsel, F. R. McFeely, A. Taleb-Ibrahimi, and J. A. Yarmoff*
IBM Research Division, Thomas J. Watson Research Center, P.O. Box 218, Yorktown Heights, New York 10598

G. Hollinger
Laboratoire d'Electronique Automatique et Mesures Electriques, Ecole Centrale de Lyon, Boîte Postale No. 163, F-69131 Ecully Cédex, France

(Received 7 March 1988)

The bonding of Si atoms at the SiO_2/Si interface is determined via high-resolution core-level spectroscopy with use of synchrotron radiation. All four oxidation states of Si are resolved, and their distribution is measured for Si(100) and Si(111) substrates. For oxides grown in pure O_2, the density of Si atoms in intermediate oxidation states is $(1.5\pm0.5)\times10^{15}$ cm^{-2}. This value is obtained by measuring the core-level intensity, the escape depth in Si and SiO_2, and the relative Si $2p$ photoionization cross section for different oxidation states. From the density and distribution of intermediate-oxidation states, models of the interface structure are obtained. The interface is not abrupt, as evidenced by the high density of intermediate-oxidation states (about two monolayers of Si) and by their nonideal distribution. The finite width of the interface is explained by the bond-density mismatch between SiO_2 and Si. The electrical properties of the interface (band lineup, Fermi, and vacuum level) are determined. Annealing in H_2 is found to influence the electrical parameters by removing the P_b centers that pin the Fermi level. The distribution of oxidation states is not affected.

I. INTRODUCTION

The SiO_2/Si interface has been the subject of intense study[1–4] because of its dominant role in silicon technology. The structure of this interface has been elusive despite many efforts to come up with models. Previous studies generally agree in identifying two distinct regions. The near interface consists of a few atomic layers containing Si atoms in intermediate oxidation states, i.e., Si^{1+} (Si_2O), Si^{2+} (SiO), and Si^{3+} (Si_2O_3). A second region extends about 30 Å into the SiO_2 overlayer. The SiO_2 in this layer is compressed because the density of Si atoms is higher for Si than for SiO_2. In this work, we will focus onto the near-interface region. Several structural models have been proposed[5–11] for SiO_2 on Si(100), each predicting a characteristic distribution of oxidation states. Most of the models published to date assume an atomically abrupt interface. From our data we can exclude such abrupt models, since they cannot explain the large portion of Si^{3+} observed at the interface. A recent calculation arrives at an extended-interface model for SiO_2/Si(100) by minimizing the strain energy.[11] This model is found to be in good agreement with our data. It is not unique, though. New models are proposed for SiO_2/Si(100) and SiO_2/Si(111) based on the distribution and intensity of intermediate-oxidation states. These models are characterized by an extended interface, with protrusions of Si^{3+} reaching about 3 Å into the SiO_2 overlayer.

Many experimental techniques have been used previously to determine the structure of the interface, its extent and its roughness, e.g., transmission electron microscopy[5,9,12–14] (TEM), scanning tunneling microscopy[14,15] (STM), low-energy electron diffraction[16] (LEED), positron annihilation,[17] ellipsometry,[18] vibrational spectroscopy,[19,20] Rutherford backscattering[21] (RBS), x-ray scattering,[22] field ion microprobe,[23] Auger spectroscopy,[24,25] and x-ray photoelectron spectroscopy (XPS).[26–43] The results range from atomically sharp to extended interfaces of about 7 Å width. These variations could be due to the different probing techniques or to the differences in sample preparation. We have ascertained that our observed interface properties hold for a wide class of oxides by covering a broad range of preparation conditions. A unique interface structure is found for the "ideal" SiO_2/Si interface, i.e., an interface in thermal equilibrium (see Ref. 44) and free of impurities, such as hydrogen or OH. The preparation conditions play a minor role as long as one starts with clean and smooth Si surfaces.

The experimental technique employed in this work is core-level spectroscopy (for a review of core-level spectroscopy at Si surfaces, see Ref. 45). It has the advantage of resolving the oxidation states[27,42] of Si atoms in the interface layer via the chemical shift of the Si $2p$ core level. Therefore, a straightforward definition of the interface can be given by taking the layer that contains Si atoms in intermediate-oxidation states. The depth resolution is optimized by using tunable synchrotron radiation. At a photon energy of 130 eV, the escape depth of photoelectrons from the Si $2p$ core level has a minimum of about 3 Å in Si, compared with about 15 Å in conventional XPS. The short escape depth makes it easy to detect a monolayer of Si atoms at the interface. For a quantitative evaluation of the core-level spectra one has to determine the

 ©1988 The American Physical Society

escape depth in SiO_2 as well as that in Si (SiO_2 has about twice the escape depth of Si). Also, the difference in the photoionization cross section between the various oxidation states has to be taken into account (the higher oxidation states have about twice the cross section of elemental Si at $h\nu=130$ eV due to a resonance effect). In this work we have determined these parameters for a range of photon energies (120–400 eV), where there is very little information available.

II. EXPERIMENT

The data were taken with a spectrometer-monochromator setup at the National Synchrotron Light Source.[45] The photoelectrons were collected within a cone of 86° full width centered around the sample normal. The light was p polarized with an angle of incidence 64° from normal. The energy resolution of the electron analyzer was set between 0.1 and 0.2 eV, and the photon energy resolution varied from 0.2 eV at $h\nu=130$ eV to 0.4 eV at $h\nu=400$ eV.

Thin SiO_2 films were obtained by oxidizing atomically clean Si surfaces in pure O_2. Clean Si(111)7$\times$7 and Si(100)2$\times$1 surfaces were prepared by Ohmic heating of Si wafers to 1050 °C or by dipping in 10% HF and heating to 850 °C. Well-oriented wafers ($<\frac{1}{4}$° misorientation) were used to obtain the data shown here, but wafers with 3° misorientation gave similar results. Using an ultrahigh vacuum transfer system, the clean Si samples were transferred from the spectrometer (pressure $<10^{-10}$ Torr) to a preparation chamber which could be filled with gases up to a pressure of 1 atm and subsequently pumped down to ultrahigh vacuum. During all oxygen exposures, the sample was cooled while still in oxygen. Thereby, the formation of holes in the SiO_2 layer is prevented, which occurs when a thin SiO_2 film is heated in vacuum (see Ref. 46). Vacuum-annealed films with pinholes exhibit a larger signal from bulk Si. The density of Si atoms in intermediate-oxidation states is underestimated when using such data. The native oxide as well as oxides grown in H_2O and by wet chemistry (HNO_3, H_2O_2) have also been studied but in a less systematic way.

Figure 1 illustrates the analysis of the data for a core-level spectrum from SiO_2/Si(100). Oxidation states intermediate between Si and SiO_2 are already visible in the raw data (top curve in Fig. 1). For a quantitative evaluation we apply three straightforward data-processing steps. The first is to subtract a secondary electron background (dashed line in Fig. 1) from the raw data. This background curve is measured separately at a 10-eV-lower photon energy where the Si $2p$ core-level structure is shifted away. A small background remains at the low-kinetic-energy side of the spectrum due to energy losses from the core lines. This background is removed in a second step by subtracting a curve proportional to the integral of the spectrum. Such a procedure is equivalent to approximating the loss function by a constant. After removing the total background (dotted line in Fig. 1) the spectrum is decomposed into the Si $2p_{1/2}$ and Si $2p_{3/2}$ spin-orbit partner lines. This decomposition is mathematically unique as long as the spin-orbit splitting and the intensity ratio are known. The splitting of 0.61 eV is an atomic property and practically independent of the chemical environment. A variation of the splitting between 0.59 and 0.61 eV has been observed by fitting the bulk Si lines. The $2p_{1/2}$ to $2p_{3/2}$ intensity ratio comes out in these fits to be equal to the statistical value of 1:2 within $\pm 2\%$. In all following figures the spin-orbit decomposed curves will be shown for clarity.

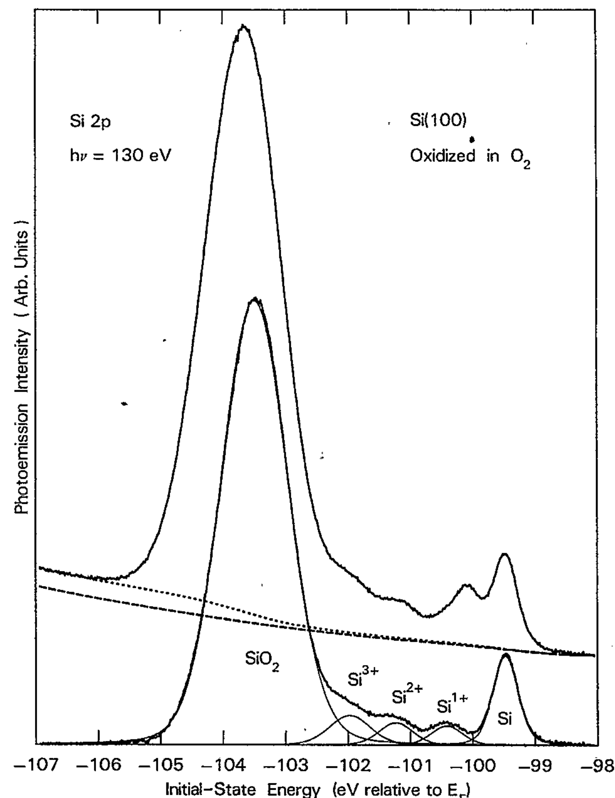

FIG. 1. Intermediate-oxidation states at the SiO_2/Si(100) interface, identified by their Si $2p$ core-level shifts. The top curve represents the raw photoemission data for the Si $2p_{1/2,3/2}$ core levels. The bottom curve has the Si $2p_{1/2}$ line and the secondary electron background subtracted. All three intermediate-oxidation states are seen. For a truncated bulk structure only Si^{2+} would be present since the Si(100) surface has two broken bonds per atom.

III. CORE-LEVEL INTENSITIES, CROSS SECTIONS, AND ESCAPE DEPTHS

In order to obtain the number of Si atoms in intermediate-oxidation states and to test structural models it is necessary to quantitatively evaluate the core-level intensities. The photoemission intensity is determined by six quantities, i.e., the atomic photoionization cross sections σ_{Si} and σ_{SiO_2}, the escape depths l_{Si} and l_{SiO_2}, and the density of Si atoms n_{Si} and n_{SiO_2} in Si and SiO_2, re-

spectively. Our experimental results for the relevant quantities are collected in Table I together with work at XPS energies.[26,30,37,74] For Si in intermediate oxidation the results fall in between the values for Si and SiO_2 as shown for the cross sections in Table II.

The core-level intensity I_{SiO_2} for a SiO_2 overlayer of thickness d is obtained by integrating over the exponential escape probability:

$$I_{SiO_2} \sim n_{SiO_2}\sigma_{SiO_2}\int_0^d \exp(-z/l_{SiO_2})dz$$
$$= n_{SiO_2}\sigma_{SiO_2} l_{SiO_2}[1-\exp(-d/l_{SiO_2})] \ . \quad (1)$$

The emission from the Si substrate is given by a similar expression except that the escape probability is multiplied by the attenuation factor $\exp(-d/l_{SiO_2})$ of the overlayer:

$$I_{Si} \sim n_{Si}\sigma_{Si}\exp(-d/l_{SiO_2})\int_0^\infty \exp(-z'/l_{Si})dz'$$
$$= n_{Si}\sigma_{Si} l_{Si}\exp(-d/l_{SiO_2}) \ . \quad (2)$$

Combining (1) and (2) we obtain, for the intensity ratio between the SiO_2 and Si core-level peaks,

$$\frac{I_{SiO_2}}{I_{Si}} = \frac{I_\infty}{I_0}[\exp(+d/l_{SiO_2})-1] \ , \quad (3a)$$

where

$$I_\infty = n_{SiO_2}\sigma_{SiO_2} l_{SiO_2}$$

and

$$I_0 = n_{Si}\sigma_{Si} l_{Si}$$

are the intensities for an infinitely thick SiO_2 layer and for a bare Si substrate, respectively. The experimental intensity ratio I_∞/I_0 is also given in Table I. It reverses between low and high photon energies. This reversal is due to a near cancellation of the factors contributing to I_∞/I_0. One finds $\sigma_{SiO_2} \geq \sigma_{Si}$ and $l_{SiO_2} > l_{Si}$ for the photon energy range considered here, which is opposite to the density ratio $n_{SiO_2} < n_{Si}$. At low photon energies ($h\nu = 130$ eV) a resonance in σ_{SiO_2} tips the intensity balance in favor of SiO_2; at high photon energies the low density of Si atoms in SiO_2 dominates over the other factors.

To determine the escape depth in SiO_2 we use a layer of known thickness d and solve Eq. (3a) with respect to l_{SiO_2}:

$$l_{SiO_2} = d \Big/ \ln\left[\frac{I_{SiO_2}}{I_{Si}}\frac{I_0}{I_\infty}+1\right] \ . \quad (3b)$$

The thickness is determined by ellipsometry on SiO_2 films of 10–30 Å thickness and checked with transmission electron microscopy (TEM). The result for the escape depth at $h\nu = 200$ eV agrees with a previous determination,[25] which used the attenuation of Si $2p$ Auger electrons by a SiO_2 overlayer and calibrated the SiO_2 thickness by nuclear analysis of the oxygen content.

For determining the escape depth in Si we use the intensity of shifted surface core levels at clean Si surfaces.[47]

TABLE I. Experimental values of the parameters required for a quantitative description of Si $2p$ core-level intensities (see Sec. III). The kinetic energy of the photoelectrons is 104 eV (108 eV) smaller than the photon energy for Si (SiO_2). The relation [Eq. (3a)] $I_\infty/I_0 = n_{SiO_2}\sigma_{SiO_2}l_{SiO_2}/n_{Si}\sigma_{Si}l_{Si}$ allows a consistency check, which gives a typical accuracy of ±10%. The results for the photon energy range up to 400 eV are from this work, the XPS results are from Refs. 30, 37, and 74. Bulk atom density: $n_{SiO_2} = 2.28\times10^{22}$ cm^{-3}, $n_{Si} = 5.00\times10^{22}$ cm^{-3}. Surface atom density of Si (1 monolayer): $N_{111} = 7.8\times10^{14}$ cm^{-2}, $N_{100} = 6.8\times10^{14}$ cm^{-2}.

$h\nu$ (eV)	$\frac{I_\infty}{I_0}$	$\frac{n_{SiO_2}\sigma_{SiO_2}l_{SiO_2}}{n_{Si}\sigma_{Si}l_{Si}}$	$\frac{\sigma_{SiO_2}{}^{a}}{\sigma_{Si}}$	l_{SiO_2} (Å)[b]	l_{Si} (Å)[b]
120	1.8	1.7	1.8[c]	8.5[d]	4.0[e]
130	2.1	2.2	2.2[c]	7.1[d]	3.3[e]
145	1.4	1.7	2.0[c]	6.3[d]	3.3[e]
200	0.84	0.77	1.3[c]	6.5,[d] 6.5[f]	5[e]
400	0.69			11[d]	10[e]
1254	0.82[g]		1.1[g]	21,[g] 25[k]	13,[g] 23[k]
1487	0.82[g]		1.1[g]	26,[g] 37[h] 36–45,[i] 27[k]	16,[g] 27,[h] 26[k]

[a]Only the adiabatic peak is considered (not the satellites).
[b]The escape depth is averaged over a 86° emission cone around the normal.
[c]From absolute core-level intensities of monolayer oxide films (Ref. 57).
[d]From the intensity ratio between oxide and substrate for samples of known thickness using Eq. (3b).
[e]From the surface core-level intensity for Si(100)2×1 assuming half a monolayer with shifted core levels (asymmetric dimer model). Compare Eqs. (4) and (5) for the analysis.
[f]From Derrien and Commandre (Ref. 25).
[g]From Hochella and Carim (Ref. 37).
[h]From Hill et al. (Ref. 30).
[i]From G. Hollinger et al. (Ref. 74).
[k]From Flitsch and Raider (Ref. 26).

TABLE II. Energy positions, widths and cross sections for intermediate-oxidation states. The width quoted is the Gaussian FWHM due to inhomogeneous broadening. The instrumental resolution is subtracted quadratically, and the lifetime broadening is accounted by a Lorentzian of 0.1 eV FWHM. Typical variations are ±5% for the energy positions and ±10% for the widths.

	Energy (eV)	FWHM (eV)	σ/σ_{Si} ($h\nu$=130 eV)
Si^0	0	0.28	1
Si^{1+}	−0.95	0.44	1.0[a]
Si^{2+}	−1.75[b]	0.58	1.1[c]
Si^{3+}	−2.48[b]	0.66	1.7[c]
Si^{4+}	−3.9[b]	1.15	2.2[c]

[a]From a comparison of surface core-level intensities for H_2O/Si(100)2×1 with clean Si(100)2×1 (compare Figs. 2 and 3).
[b]The Si^{4+} core level moves up for films thinner than 5 Å due to a smaller valence-band offset and extra screening by the Si substrate. The Si^{3+} and Si^{2+} core levels move down for films thinner than 5 Å due to the absence of dielectric screening by the SiO_2 overlayer.
[c]From absolute core-level intensities of monolayer oxides films (for details see Ref. 57).

For this purpose, we calculate the intensity from the outermost Si layer relative to the total core-level emission. It is convenient to sum the intensities layer by layer rather than integrating over a continuum as in Eqs. (1) and (2). [In a continuum model one runs into difficulties in defining the boundaries between layers when the layers are not equally spaced, such as for Si(111). With equidistant layers the continuum and the discrete models give identical results, e.g., for Si(100).] Between layers one has an attenuation factor

$$q_{hkl}=\exp(-d_{hkl}/l), \quad l=l_{Si},l_{SiO_2},l_{SiO_x}, \tag{4}$$

with an interlayer spacing $d_{100}=a/4=1.36$ Å for Si(100) and two alternating interlayer spacings $d_{111}=a\sqrt{3}/12=0.784$ Å and $d'_{111}=3d_{111}$ for Si(111). The intensity from all Si layers can easily be summed up as a geometric series $\sum_{n=0}^{\infty} q_{hkl}^n=1/(1-q_{hkl})$. The intensity of the surface layer relative to the total intensity is

$$R_{100}=(1-q_{100}) \tag{5a}$$

for a Si(100) surface,

$$R_{111}=(1-q_{111}^4)/(1+q_{111}) \tag{5b}$$

for Si(111) truncated between double layers (one broken bond), and

$$R'_{111}=(1-q_{111}^4)/(1+q_{111}^3) \tag{5c}$$

for Si(111) truncated inside a double layer (three broken bonds). If one wants to apply a continuum model to the Si(111) surface one has to use an average layer spacing $d''_{111}=2d_{111}$ in order to integrate over slabs of equal thickness. The resulting ratio

$$R''_{111}=(1-q_{111}^2) \tag{5d}$$

applies to both types of Si(111) surfaces. This value differs by up to ±10% from Eqs. (5a) and (5b) at the minimum escape depth.

Surface core-level data are shown in Fig. 2 for clean Si(100)2×1 and Si(111)7×7. For Si(100)2×1 there is a surface core-level emission at 0.5 eV above the bulk line with the intensity ratio R = surface/(surface + bulk) = 0.17 at $h\nu$=130 eV. The surface emission is assigned to half a layer of outer dimer atoms using the asymmetric dimer model.[47–49] For Si(111)7×7 there is a surface line at 0.8 eV above the bulk line with the intensity ratio surface/(surface+bulk)=0.05 at $h\nu$=130 eV. It is assigned to $\frac{7}{49}$ of a monolayer of so-called rest atoms, which are negatively charged[49] according to scanning tunneling spectroscopy[50] and self-consistent calculations.[51] Applying Eqs. (4), (5a), and (5b) to these intensity ratios one obtains an escape depth of 3.3 Å (3.2 Å) from the dimer atoms (rest atoms), respectively. Well-defined Si core-level shifts are also found for adsorbate overlayers and interfaces, e.g., As/Si(111) with an intensity ratio R = surface/(surface + bulk) = 0.40 (Ref. 52), and CaF_2/Si(111) with a surface/(surface + bulk) ratio of 0.39–0.46 (see Fig. 3 and Refs. 53–55). Using Eq. (5c) [Eq. (5b)] one obtains escape depths of 3.4 Å (2.9–2.1 Å) for As/Si(111) [CaF_2/Si(111)]. However, the analysis of

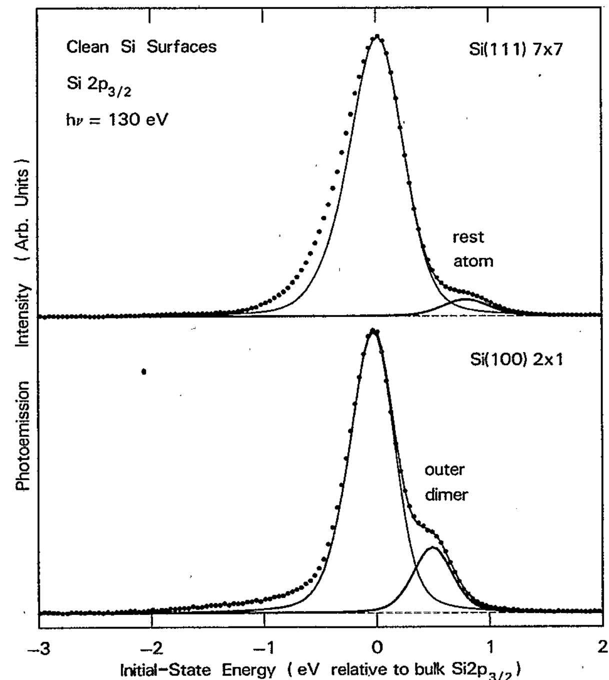

FIG. 2. Core-level spectra from clean Si(100)2×1 and Si(111)7×7 surfaces used for determining the escape depth in Si. The emission from shifted surface core levels correspond to $\frac{1}{2}$ and $\frac{1}{7}$ of a monolayer, respectively. Energy-loss features below the bulk lines are not included in the fit.

the core-level intensities may be affected in this case by a change in cross section due to chemical bonding (see below). In summary, the escape depths for SiO_2 and Si exhibit a minimum for photon energies around $h\nu=140$ eV. The escape depth for SiO_2 is longer than that for Si, in agreement with theoretical estimates.[56]

In addition to the escape depth there is another factor that influences the core-level photoemission intensity, i.e., the photoionization cross section. Previously, it has been assumed that the cross section is identical for all oxidation states of Si at a given photon energy. It turns out that this is far from being true for the photon energy range in question. Near $h\nu=130$ eV there is a shape resonance in the cross section for the higher oxidation states which causes them to be enhanced by up to a factor of 2. This cross section resonance diminishes as one approaches lower oxidation states (corresponding to lower core-level shifts). Therefore, we expect only minor cross section effects for the clean Si surface core levels, for As/Si(111) and for CaF_2/Si(111). Our results are summarized in Tables I and II. The cross section ratios are obtained by photon-energy-dependent measurements of the absolute core-level intensities of Si^{1+},Si^{2+},Si^{3+},Si^{4+}. Thereby we use very thin films (monolayer or less) in order to minimize the effect of the photon-energy-dependent escape depth. The Si^{1+} cross section is referred to the Si cross section by comparing the Si^{1+} peak at the H_2O-exposed Si(100) surface with the surface core-level emission at the clean surface (see discussion of Figs. 2 and 3). A detailed account of the cross-section measurements will be published elsewhere.[57]

IV. NUMBER OF INTERFACE ATOMS

An important quantity is the number of N_{SiO_x} of Si atoms in intermediate-oxidation states (per unit area). In order to get a rough idea we compare in Fig. 3 core-level spectra of two reference structures with SiO_2/Si(111). The Ca-terminated CaF_2/Si(111) interface[53–55] has about a monolayer of Si atoms bonding to Ca giving rise to a shifted core level located 0.4 eV above the bulk line. Some residual Si—F bonds show up on the low-energy side of the bulk line. For our purpose the H_2O-exposed Si(100)2$\times$1 surface is better suited since it takes a possible change in cross section from elemental Si to oxidized Si into account. This surface exhibits a surface core level at 0.9 eV below the bulk line corresponding to 0.5 monolayers (Ref. 58) of Si^{1+}. The intensity measured for saturation coverage (about 20 L) is $Si^{1+}/(Si^0+Si^{1+})=0.17$. It has been assigned[59] to 0.5 monolayers of OH bonding to Si. The other half of the Si surface atoms bond to H and exhibits a much smaller shift of 0.3 eV. They have been included in the bulk line. The Si^{1+} peak for SiO_2/Si(111) has an intensity ratio $Si^{1+}/(Si^0+Si^{1+})=0.30$ at $h\nu=130$ eV, i.e., 1.8 times greater than for the H_2O/Si(100) reference surface. From there we determine a coverage of 0.87 monolayers of Si^{1+} for SiO_2/Si(111). Thereby the small change in the surface-to-bulk ratio due to the difference surface orientation has been taken into account.[60] The coverage of the higher-oxidation states is more difficult to determine since their intensity is

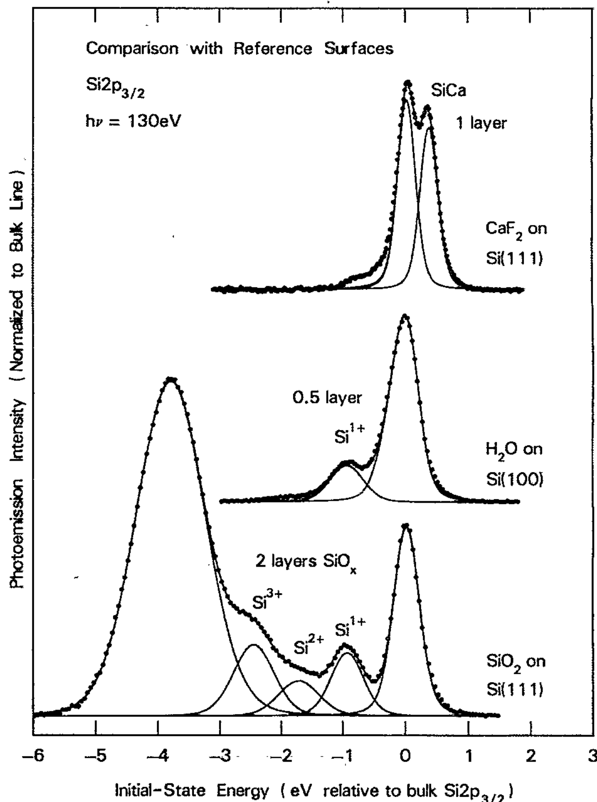

FIG. 3. Comparison of core-level spectra from SiO_2/Si(111) with the CaF_2/Si(111) interface and the H_2O-exposed Si(100)2$\times$1 surface. A density of two Si layers is derived for the Si atoms in intermediate-oxidation states by comparing with the H_2O/Si(100) reference surface.

enhanced relative to Si^{1+} at a photon energy of 130 eV. Two effects contribute to this enhancement. One is a resonance in the cross section of Si^{3+} at this photon energy (see discussion in Sec. III and Table II), the other is an escape depth effect caused by the fact that Si^{3+} is farther away from the Si substrate than Si^{1+} (see Sec. V). In order to become free of these distortions it is helpful to use data at higher photon energies ($h\nu=400$ eV in our case) where the cross sections are nearly the same and the mean free path is significantly larger than the width of the interface. In this case the true distribution of oxidation states is seen. From the data for $h\nu=400$ eV in Table III we find that the total number of Si atoms in intermediate oxidation states is 2.6 times that of Si^{1+}, i.e., 2.3 Si(111) monolayers. This corresponds to 1.8×10^{15} atoms/cm^2. A somewhat smaller value of 1.3×10^{15} atoms/cm^2 (i.e., 1.9 Si(100) monolayers) is obtained for SiO_2/Si(100) by comparing the $(Si^{1+}+Si^{2+}+Si^{3+})/Si^0$ intensity ratios for Si(100) and Si(111) at $h\nu=400$ eV (see Table III). It is interesting to note that the SiO_2/Si(100) interface also has a lower density of dangling bond defects (P_b centers[61,62]) than Si(111). Thus, there seems to be a correlation between the density of intermediate-oxidation states and the density of P_b centers. The absolute number of P_b centers is 3 orders of magnitude lower, though. A similar correlation between the density of

TABLE III. Relative intensities of intermediate-oxidation states for SiO_2/Si(100) and SiO_2/Si(111). The intensities are obtained by a least-squares fit to the data with the energies and widths constrained to the values given in Table II. Typical variations between samples are ±10% for $I^{1+}:I^{2+}:I^{3+}$, and up to 30% for I^0. In order to obtain the true distribution of oxidation states, the intensities have to be divided by the respective cross sections (given in Table II for $h\nu=130$ eV).

$h\nu$ (eV)	$\frac{I^{3+}}{I^{1+}+I^{2+}+I^{3+}}$	$\frac{I^{2+}}{I^{1+}+I^{2+}+I^{3+}}$	$\frac{I^{1+}}{I^{1+}+I^{2+}+I^{3+}}$	$\frac{I^{0}}{I^{1+}+I^{2+}+I^{3+}}$
		Si(111) data		
120	0.41	0.25	0.34	0.95
130	0.48	0.21	0.31	0.74
145	0.48	0.21	0.31	0.77
400	0.33	0.29	0.38	2.7
		Si(100) data		
130	0.48	0.28	0.24	1.1
400	0.37	0.35	0.28	3.6

intermediate-oxidation states and the electrically active interface states has been observed in the oxidation of SiGe alloys.[63]

There is an independent way to obtain the number of intermediate-oxidation states by using only data taken at $h\nu=400$ eV. At this photon energy the depth distribution of intermediate-oxidation states does not matter. It can be modeled by a constant density n_{SiO_x} over a width δ. Equation (3a) can be generalized to give the intensity ratio between intermediate-oxidation states and the Si substrate:

$$\frac{I_{SiO_x}}{I_{Si}}=\frac{n_{SiO_x}\sigma_{SiO_x}l_{SiO_x}}{n_{Si}\sigma_{Si}l_{Si}}[\exp(+\delta/l_{SiO_x})-1] . \quad (6)$$

For $\delta \ll l_{SiO_x}$, the last factor becomes δ/l_{SiO_x}. The number of Si atoms in intermediate-oxidation states per unit area is then

$$N_{SiO_x}=n_{SiO_x}\delta=\frac{I_{SiO_x}}{I_{Si}}\frac{\sigma_{Si}}{\sigma_{SiO_x}}n_{Si}l_{Si} . \quad (7)$$

The experimental ratio is $I_{SiO_x}/I_{Si}=(I^{1+}+I^{2+}+I^{3+})/I^0=0.37$ and 0.28 at $h\nu=400$ eV for Si(111) and Si(100), respectively (see Table III). Assuming $\sigma_{Si}/\sigma_{SiO_x}\doteq 1$ at $h\nu=400$ eV and using $l_{Si}=10$ Å, $n_{Si}=5\times10^{22}$ cm^{-3} (Table I) one obtains for the number of Si atoms in intermediate oxidation states $N_{SiO_x}=1.9\times10^{15}$ cm^{-2} on Si(111) [$N_{SiO_x}=1.4\times10^{15}$ cm^{-2} on Si(100)]. These values are comparable with the results obtained in the preceding paragraph from comparison with reference spectra. The accuracy is less due to a relatively large uncertainty in the determination of l_{Si} at $h\nu=400$ eV and due to the possible contribution of a satellite emission at about 1.5 eV below the bulk Si line.[64] It is clear from the two independent measurements that the density of intermediate-oxidation states at the SiO_2/Si interface is about two silicon layers, i.e., twice of that expected for an atomically abrupt interface.

V. DISTRIBUTION OF OXIDATION STATES

In the Si 2*p* core-level spectra shown in Figs. 4 and 5 one can clearly identify three peaks between the Si and the SiO_2 lines, which correspond to the three possible intermediate-oxidation states Si^{1+},Si^{2+},Si^{3+}. One should

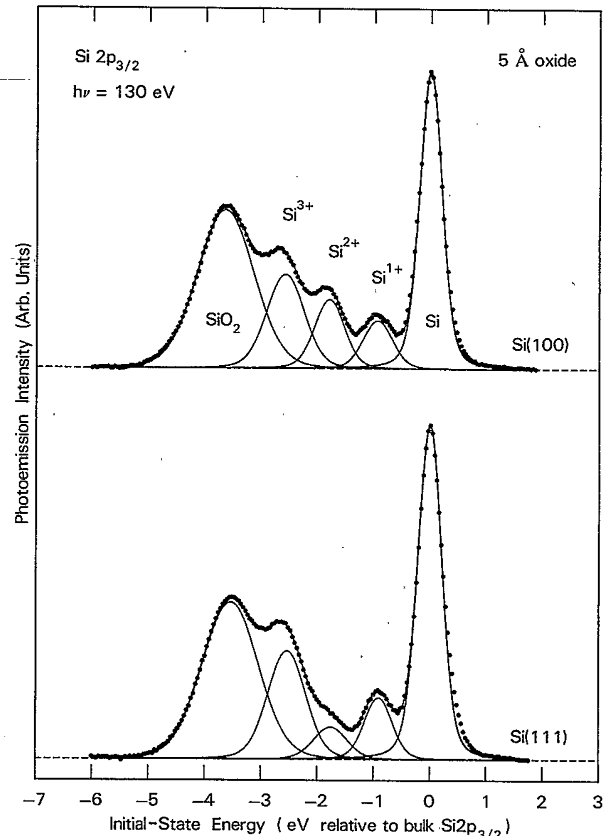

FIG. 4. Core-level spectra from ultrathin SiO_2 overlayers on Si(100) and Si(111) surfaces. The Si(111) substrate has less Si^{2+} and more Si^{1+} than the Si(100) substrate. Si^{3+} is enhanced by a factor of 1.7 at this photon energy due to a cross-section resonance (see Table II). The films were grown in 2×10^{-5} Torr O_2 at 750 °C for 20 sec.

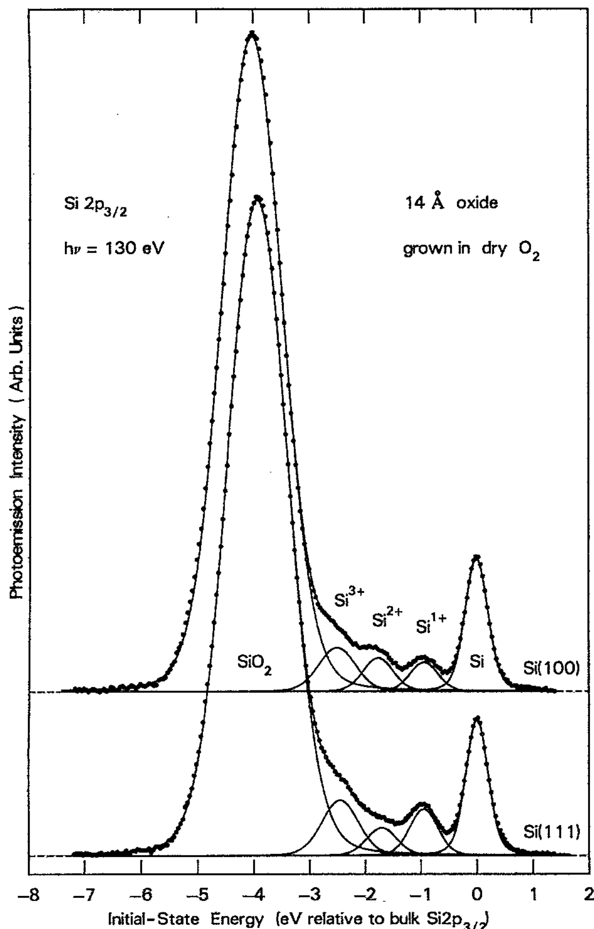

FIG. 5. Core-level spectra from intermediate SiO_2 overlayers on Si(100) and Si(111). The distribution of oxidation states is similar to that for ultrathin layers. The films were grown in 0.1 Torr O_2 at 850 °C for 10 sec.

keep in mind that these symbols refer to the oxidation state, not to the actual charge transfer. The charge transfer is only about half an electron per oxidation state.[27,65] The energy positions and the widths of the core lines are given in Table II. Figures 4 and 5 compare Si $2p_{3/2}$ core-level spectra for SiO_2 films of different thickness. The absolute intensity of intermediate-oxidation states goes down with increasing film thickness due to attenuation by the SiO_2 overlayer. For films thicker than about 30 Å the interface signal decreases below the detection limit. This observation rules out the existence of Si atoms in intermediate-oxidation states at the surface. The intensity distribution of intermediate-oxidation states, $I^{1+}:I^{2+}:I^{3+}$, does not vary much with the oxide overlayer thickness, showing that this is a universal property of the SiO_2/Si interface. Results obtained from least-squares fitting are given in Table III. Also, the intensity of intermediate-oxidation states relative to that of the Si substrate (I^0) is given. It is generally independent of the layer thickness. However, it can be affected in both ways by poor sample preparation. Pinholes due to vacuum annealing of thin SiO_2 films cause the Si signal to increase. Rough starting surfaces, on the other hand, produce more intermediate-oxidation states.

Several processing parameters have been varied in order to test the universal nature of SiO_2/Si interface. Pressure and temperature variations (from 10^{-5} to 20 Torr and from 700 to 1100 °C, respectively) do not affect the distribution of oxidation states significantly. This finding holds for a film thickness of up to 30 Å which is the upper limit for our probing technique. Thicker films may be studied by back-etching with HF (see Refs. 2, 29, and 33), but at the risk of altering the stoichiometry and creating holes with H-terminated[20,66,67] Si. For very thin oxide films (8 Å or less) the intensity of intermediate-oxidation states is found to decrease relative to the bulk line although their distribution remains unchanged. It is likely that these films are not continuous, giving rise to extra emission from clean Si through pinholes. Oxidation at room temperature leads to distributions with a larger proportion of the lower oxidation states (Si^{1+} is the strongest component). This holds for oxidation in dry oxygen[39,41,68] as well as in oxidizing solutions[69] (e.g., HNO_3). These films have a structure different from the high-temperature oxides. The models in Refs. 9 and 10 predict exclusively Si^{1+} at the interface, in qualitative agreement with the room-temperature data. We will not discuss room-temperature oxidation in detail, as we are mainly concerned with the structure obtained at elevated temperature in thermal equilibrium.[44] It has been shown for very thin oxides[41] that the room-temperature distribution converts to the universal high-temperature distribution after annealing at 700 °C in vacuum. Recently, thicker oxide films have been grown at room temperature on very flat molecular-beam epitaxy (MBE) Si(100) substrates,[9,68] which exhibit a dominant Si^{1+} state.[68] When these structures are heated in vacuum, the abundance of higher oxidation states increases. Very rough or defective surfaces produce a larger density of intermediate-oxidation states. Such surfaces are produced by heating Si(100) above 1100 °C, or in the presence of impurities. They are characterized by weak surface core-level signals. We have also looked into the effect of H_2 annealing on the distribution of intermediate-oxidation states (see Sec. VII). There is no noticeable difference. This is understandable since the number of dangling bonds (P_b centers) that can be saturated by hydrogen reaches at most about 10^{12} cm^{-2} (Ref. 61), i.e., $\frac{1}{1000}$ of a monolayer. Such small changes are not detectable with our technique. The presence of H_2, e.g., in steam oxidation, has been reported[2,29] to give rise to an abrupt interface where 6–17 % of the interface bonds are saturated by H. In this case the higher temperature may cause the strong Si—O—Si bridge bonds to break up (compare also the discussion in Sec. VIII). Annealing in atomic hydrogen has also been reported[2] to cause incorporation of substantial amounts of H in the interface. This may be explained by the high reactivity of atomic versus molecular hydrogen. In the following we will concentrate on the pure SiO_2/Si interface that is formed in the absence of hydrogen.

In Figs. 4 and 5 the distribution of intermediate-

oxidation states is shown for two crystallographic orientations of the substrate. All three intermediate-oxidation states are present for Si(111) as well as for Si(100), but their intensity ratios are different. On Si(100) the Si^{1+}, Si^{2+}, and Si^{3+} states appear in roughly equal proportion, on Si(111) the Si^{2+} state is suppressed. This crystallographic trend can be explained by the bond topology of the truncated bulk structure. A Si(111) surface can have two types of crystallographic planes with one and three broken bonds per atom, respectively, which give rise to Si^{1+} and Si^{3+} when saturated by oxygen. The Si(100) surface has two broken bonds per atom, which give rise to Si^{2+}. The coexistence of all three oxidation states on Si(100) clearly indicates deviations from the ideal, atomically abrupt interface.

In order to pin down the structure of the interface it is helpful to obtain a clue about the depth distribution of various oxidation states. This can be done by changing the escape depth, either by changing the take-off angle of the photoelectrons (see Refs. 30, 31, 35, and 36) or by varying the photon energy (see Fig. 6; compare also Refs. 28 and 32). At a photon energy $h\nu=130$ eV the outer portion of the interface is enhanced due to the small escape depth, whereas at $h\nu=400$ eV it is given the same weight as the deeper regions of the interface. A least-squares fit to the data (see Table III) shows that, indeed,

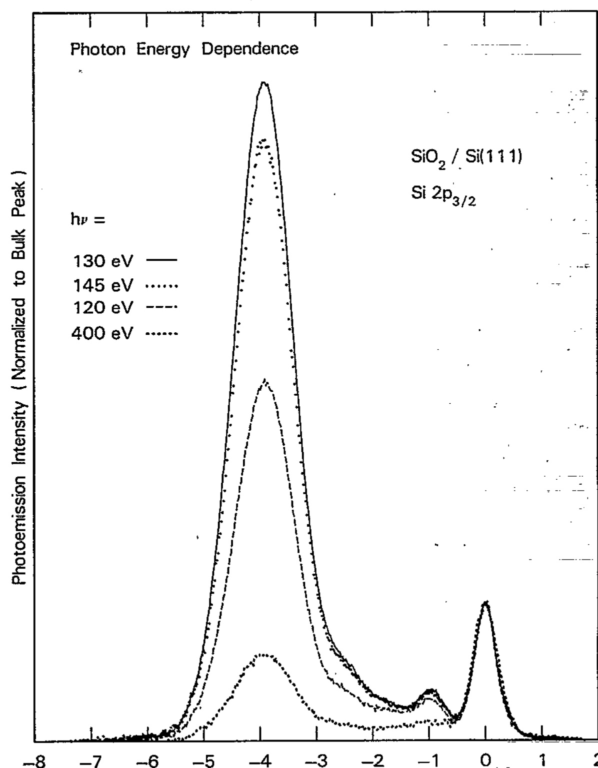

FIG. 6. Core-level spectra vs photon energy $h\nu$ for 14 Å oxide on Si(111). At $h\nu=130$ eV there is a minimum in the escape depth as evidenced by the maximum in the SiO_2/Si intensity ratio. The Si^{3+} contribution is enhanced at this photon energy relative to Si^{1+} and Si^{2+}. The enhancement is partly due to the fact that Si^{3+} is closer to the surface and partly due to a cross section resonance of Si^{3+} at this photon energy.

the Si^{3+} intensity increases significantly relative to Si^{2+} and Si^{1+} at $h\nu=130$ eV. Therefore, one would want to conclude that the Si^{3+} atoms must be located farther out than Si^{2+} and Si^{1+}, as expected from the kinetics of the oxidation process. However, the enhancement of Si^{3+} at $h\nu=130$ eV is largely caused by a cross-section resonance (see Sec. III). After dividing the intensities by the cross-section factors given in Table II one obtains relative intensities of $I^{3+}:I^{2+}:I^{1+}=0.36:0.24:0.40$ at $h\nu=130$ eV for Si(111). This is already very close to the ratios $I^{3+}:I^{2+}:I^{1+}=0.33:0.29:0.38$ at $h\nu=400$ eV, where cross section and escape depth effects are absent. Therefore, it is difficult to extract quantitative depth information. Recent depth-profiling work[35] uses angle-dependent XPS data, which are transformed into a depth distribution by an inverse Laplace transform. Si^{3+} is found to be 6–10 Å farther away from the interface than Si^{2+}, somewhat more than expected from our structural models. We note that previous depth-profiling work[28–33] gives information about a larger length scale. A small concentration of Si^{3+} (a few percent) is found to be distributed over a depth of 30 Å or more inside the SiO_2 film.

VI. INTERFACE STRUCTURE

A coarse look at the distribution of oxidation states gives two qualitative results about the structure of the interface. (i) The interface is not ideal, as evidenced by the coexistence of all three intermediate-oxidation states Si^{1+},Si^{2+},Si^{3+}. With a truncated bulk structure one would obtain only Si^{2+} for Si(100), and Si^{1+} or Si^{3+} for Si(111). (ii) However, there is a remnant of the crystallographic dependence expected from a truncated bulk structure. Can these findings be made consistent? In order to come up with sensible models we have to consider the possible driving forces for the interface structure. A critical boundary condition is the density mismatch between SiO_2 and Si. The SiO_2 lattice has a density of Si atoms that is 2.2 times lower than that in Si. Consequently, a SiO_2 surface has only half as many open bonds as a Si surface. In the following we will discuss how this difference can be accommodated.

First, the SiO_2/Si(100) interface is considered. The truncated bulk structure can be connected to an amorphous SiO_2 network as shown by Pantelides *et al.*[7] Such a model has a full monolayer of Si atoms in the 2+ oxidation state. An epitaxial model by Herman *et al.*[6] (Fig. 7) has the density difference between SiO_2 and Si built in. This model uses a diamondlike structure of SiO_2, which is obtained by straightening the Si—O—Si bonds in the β-cristobalite structure. The bond-length ratio between Si—O—Si and Si—Si is close to $\sqrt{2}$. Therefore, an epitaxial $(\sqrt{2}\times\sqrt{2})R45°$ structure can be constructed on Si(100). In this case, the bond density across the interface changes by a factor of 2. As shown in Fig. 7, only half of the atoms at the Si(100) surface are connected to oxygen in SiO_2. To absorb the remaining broken bonds one has to introduce impurities such as H, F, and OH at the interface. This situation may exist in high-temperature steam oxidation or in wet chemical oxidation. Alternatively, oxygen atoms may form double bonds with the

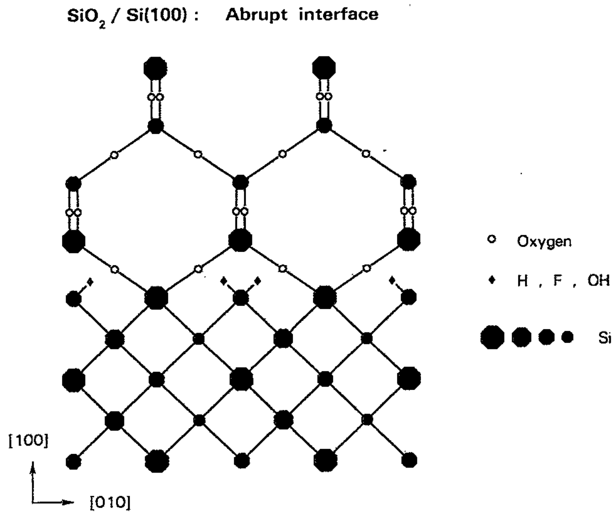

FIG. 7. Epitaxial model of the SiO_2/Si(100) interface after Herman *et al.* (Ref. 6). The mismatch in bond density at the interface prevents half of the broken bonds at the Si(100) surface from being connected with SiO_2. This density mismatch presents the major constraint in constructing structural models of the interface.

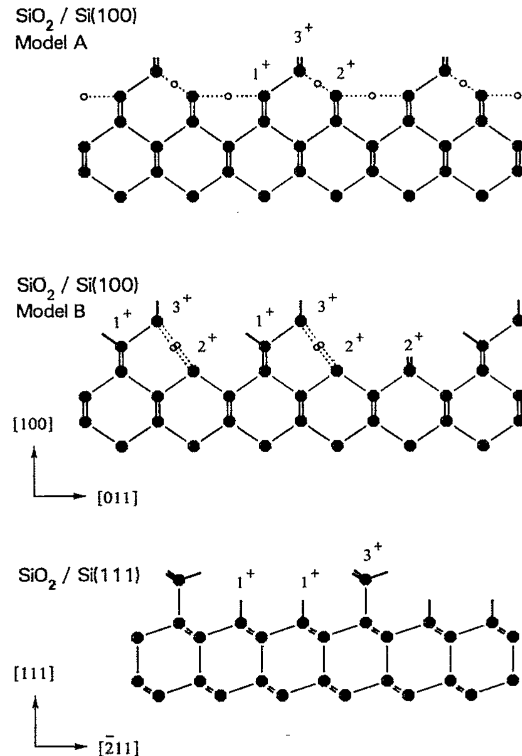

FIG. 8. Models of the SiO_2/Si(100) and SiO_2/Si(111) interfaces that match the distribution of intermediate-oxidation states. Model A is similar to a structure proposed by Ohdomari *et al.* (Ref. 11) based on strain-energy minimization. These models are characterized by Si^{3+} protrusions into the SiO_2 overlayer. Open bonds are to be connected to a SiO_2 network via oxygen bridge bonds. The bond topology is given without taking relaxation into account.

free Si surface atoms. The distribution of oxidation states expected at such interfaces is 0.5–1.0 monolayer of Si^{2+} and 0.5–0.0 monolayer of Si^{1+}. Thereby, Si atoms bonding to hydrogen are counted as Si^0. An alternative way to take care of the density mismatch has been proposed recently by Ourmazd *et al.*[9] Only one of the two broken bonds of the Si surface atoms is connected to SiO_2. The other is presumed to pair up with a neighboring Si atom in a 2×1 structure, as on the clean Si(100) surface. This configuration matches tridymite, another crystalline modification of SiO_2. The interface consists of a full monolayer of Si^{1+} for this model. In a variation of this model, one may obtain Si^{2+} by inserting oxygen into the Si—Si dimer bond. A third possibility to fix the bond density mismatch has been proposed by Ohdomari *et al.*[10,11] The Si(100) surface is terminated by Si(111) facets with one broken bond per atom, resulting in about a monolayer of Si^{1+} at the interface. All these atomically abrupt interface models give only Si^{2+} and Si^{1+} as intermediate-oxidation states.[70] A look at the bond topology of the Si(100) surface shows that the common defects (e.g., adatoms, vacancies, steps) also produce only Si^{2+} and Si^{1+}, but not Si^{3+}. In order to explain the observed Si^{3+} peak we have to resort to extended-interface models.

A solution to the density-mismatch problem is a graded interface which is 2–3 atomic layers wide (see Fig. 8). Strain energy calculations show that a properly graded SiO_2/Si(100) interface[11] has a significantly lower strain energy than an abrupt one. A specific model has been proposed by Ohdomari *et al.*[11] based on strain-energy minimization (Fig. 8, model A). We add a second structure (Fig. 8, model B), which agrees equally as well with our data. A peculiar feature common to these two models is the occurrence of Si^{3+} protrusions into the SiO_2 layer. The spacing of Si^{3+} protrusions can be estimated by fitting the observed $[Si^{3+}]/[Si^{2+}]$ ratio at $h\nu=400$ eV (see Table III). It comes out to be somewhat more than two Si lattice spacings. It is interesting to look at this spacing in terms of a misfit dislocation picture. An areal density mismatch of 1.7 is obtained from the bulk densities of SiO_2 and Si given in Table I, i.e., there are 1.7 times as many Si atoms per unit area as SiO_2 molecules. One can match this ratio by introducing dislocations in a linear array, such as for the models shown in Fig. 8. To get the proper density ratio one needs 2–3 Si lattice spacings between the dislocations (two Si atoms for one SiO_2 would give a density ratio of 2.0, three Si atoms for two SiO_2 would give a density ratio of 1.5). This is close to the experimental result, thereby supporting the view of Si^{3+} protrusions as the cores of misfit dislocations.

The SiO_2/Si(111) interface can be modeled in the same spirit (Fig. 8, bottom). The reasoning for an extended interface is not as clear, as for Si(100). The bond topology of the Si(111) surface is characterized by a double-layer structure, where layers with one broken bond alternate with layers with three broken bonds to give an average of two broken bonds per atom, as on the Si(100) surface. Taking the layer with one broken bond as interface layer

would give about the right bond density for attaching SiO_2. Strain calculations[10,11] confirm this simple bond-counting argument by giving less strain energy for the abrupt (111) interface than for the abrupt (100) interface. The experimental distribution does indeed exhibit Si^{1+} as the strongest component. However, there is a large Si^{3+} component that would create a high bond density if the interface was abrupt. In addition, the total number of Si atoms in intermediate-oxidation states is about two layers [higher even than for Si(100)]. These features can only be accommodated by an extended interface. A highly simplified model is given in Fig. 8. It does not exhibit Si^{2+}, and the number of interface atoms is too small, but these deficiencies can easily be corrected by adding steps or other defects.

VII. ELECTRICAL PROPERTIES

Some of the parameters that determine the electrical properties of the SiO_2/Si interface can be probed with photoelectron spectroscopy, e.g., the Fermi-level position in the gap, the valence-band offset, and the vacuum level. A summary of the results is given in Figs. 9 and 10 for

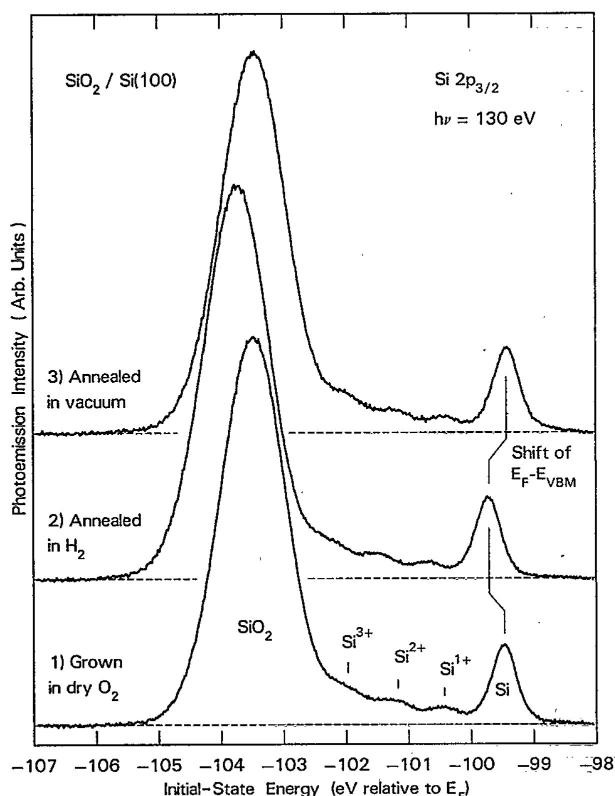

FIG. 9. Effect of H_2 annealing (1 atm H_2, 850 °C, 10 sec) on the SiO_2/Si(100) interface. A rigid shift of the whole spectrum is caused by the Fermi level moving from a pinned position to its bulk position (see Fig. 10). The distribution of oxidation states does not change, however, since the number of pinning defects is too small to be detected. Subsequent annealing in vacuum (850 °C, 1 min) restores the pure interface by driving off hydrogen.

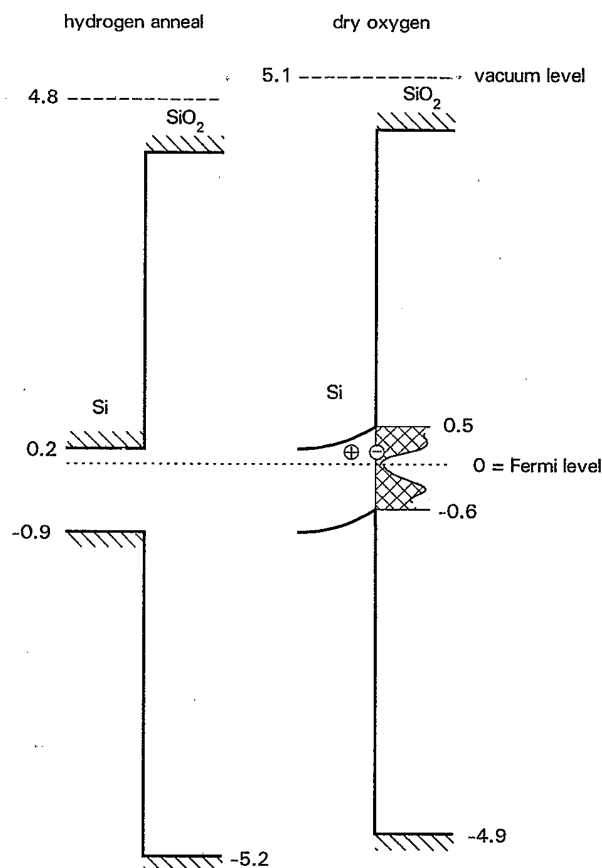

FIG. 10. Band diagram for the SiO_2/Si(100) interface corresponding to the data in Fig. 9. After dry oxidation, the Fermi level is pinned at 0.6 eV above the valence-band maximum of Si, i.e., near the neutral point of the distribution of P_b centers (taken from Johnson *et al.*, Ref. 61). Annealing in H_2 brings the Fermi level to its bulk position (shown for a 5×10^{15}-cm^{-3} *n*-type doping).

the SiO_2/Si(100) interface. The position of the Fermi-level E_F relative to the valence-band maximum E_{VBM} of Si is obtained by a method described in Ref. 71. Essentially, the position of the bulk Si 2*p* line below E_F is compared with that of a reference surface with known Fermi-level position. As such we use the CaF_2/Si(111) interface, where the Fermi level coincides with the valence-band maximum.[54] The valence-band edge has a fixed distance from the Si 2*p* level, independent of the Fermi-level position. Thus, the difference in the Si 2*p* energies reflects the difference in the valence-band maxima, measured relative to E_F. The band offset is determined from a photoelectron spectrum of the valence-band region (not shown). The conduction-band offset is obtained from the valence-band offset by adding the respective band gaps (1.1 eV for Si and 9.3 eV for SiO_2, see Ref. 72). The vacuum level is obtained from the low-energy cutoff of the photoelectron spectrum.

The electrical parameters of the SiO_2/Si interface depend on the preparation method as shown in previous

work.[2,73] We focus on the effect of annealing in hydrogen. Such a treatment is known to reduce the density of interface states.[2,61,62] Essentially, the hydrogen saturates free Si bonds (P_b centers) at the interface. Thereby the Fermi level becomes unpinned, and the band bending disappears, in agreement with our result. The Fermi-level movement shows up as an overall shift of the core-level spectrum (see Fig. 9). The shift reverses after annealing in vacuum, whereby the H is driven out. It is interesting to compare the observed pinning position of the Fermi level with the distribution of P_b centers as measured by Johnson *et al.*[61] by deep-level transient spectroscopy by (DLTS) (Fig. 10). It coincides with the neutral point between donorlike and acceptorlike centers. Such a pinning position is expected for a nearly intrinsic substrate. Another noteworthy point is that the band offset and the ionization energy (vacuum level minus valence-band maximum) do not change significantly upon H_2 annealing. This is understandable since these are intrinsic properties which are not affected by a small number of P_b centers. The barrier (conduction-band minimum minus Fermi level for *n*-type material) and the work function (vacuum level minus Fermi level) change, because the Fermi level moves relative to the band structure. The Fermi-level movement is given by the dipole that is formed between the electrons in the P_b centers and the ionized donors in the depletion region.

VIII. COMPARISON WITH OTHER RESULTS

The SiO_2/Si interface has been probed by many techniques. The interface widths reported in the literature range from abrupt to more than 7 Å wide. These variations may reflect different preparation conditions. However, it is quite clear that various measurement techniques probe different aspects of the interface. Many methods, for example, cannot resolve the atomic structure but see some average. Other techniques require intrusive sample preparation methods, such as depth profiling by sputtering or etching. Such treatments alter the chemistry of the interface.

First we discuss core-level spectroscopy results. They can be classified into two groups, i.e., XPS measurements[26–37] with a probing depth of about 30 Å and synchrotron radiation results[38–43] near the minimum of the escape depth (3–5 Å). Our photon-energy-dependent measurements bridge the gap in probing depth. There is also a difference in the sample preparation. The surface-sensitive synchrotron measurements have been performed on ultrathin (5–30 Å) SiO_2 films grown *in situ* with pure O_2 at low pressures (10^{-5} Torr). The XPS results have been obtained mainly from thick (100–1000 Å) SiO_2 films grown under device processing conditions (atmospheric pressure of oxygen or steam). These thick oxides are chemically thinned in order to see a signal from the interface. There exist a few discrepancies between the XPS and synchrotron results that need to be reconciled. An abrupt interface has been observed with XPS,[29,33] i.e., one monolayer or less (83–94 % of a monolayer[29]) of Si atoms in intermediate-oxidation states. The missing fraction of Si interface atoms has been assumed to bond to hydrogen, which comes in during steam oxidation or hydrogen annealing. Synchrotron measurements[42,43] have reported an extended interface ($\approx$5 Å wide) with about two layers of Si in intermediate-oxidation states. The easiest way to reconcile the results would be to assume that pure SiO_2 and device oxides exhibit different interface structures. Using XPS, however, we have found no significant differences in the interface-to-bulk Si 2*p* intensity ratio between oxides grown in pure O_2 at low pressure and under device processing conditions (see Ref. 74). Even chemical thinning (from 150 to 30 Å) did not affect this ratio. Furthermore, our XPS data are similar to previous XPS results reported, e.g., by Grunthaner *et al.*[29] The main differences appear to be due to the evaluation of the XPS data. In Ref. 29 an asymmetric line shape is used for bulk Si, which takes away intensity from Si^{1+} and, therefore, reduces the intensity of intermediate-oxidation states. In addition, a different formula is used in Ref. 29 to convert the intensity of intermediate oxidation states into the density of interface atoms. This conversion depends on the knowledge of the proper escape depth and density of SiO_x.

Techniques other than core-level spectroscopy will be touched upon briefly to point out which aspects of the SiO_2/Si interface they probe. The field ion microprobe[23] probes the Si/O ratio atom by atom. The interface is defined the same way as in core-level spectroscopy, i.e., the region containing Si in intermediate-oxidation states. A width of 3–5 Å is obtained[23] which is comparable with our core level result. The two layers of interface atoms that we find corresponds to 3 Å of pure Si or to 6 Å of SiO_2. An interface layer of 7±2 Å $SiO_{0.4}$ has been reported by ellipsometry.[18] These measurements rule out an abrupt interface, in agreement with our findings. Rutherford backscattering[21] is capable of determining the Si/O stoichiometry and the number of Si atoms displaced from lattice sites. Between 1.4 and 2.3 monolayers of Si atoms are found to be displaced from their lattice sites. Up to 1 monolayer of these can be attributed to an oxide with average stoichiometry SiO at the interface with 0.8–1.7 monolayers of displaced Si atoms remaining.[21] The one monolayer of SiO is only about half as much as the number of Si atoms in intermediate oxidation states that we find, but by assigning more of the displaced Si atoms as part of the interface layer one may be able to make the two results consistent. Transmission electron microscopy has been used extensively to determine the extent of the interface and to detect irregularities. The width of the interface is difficult to define in this case. Instead, various types of roughness parameters[12,13] have been used to characterize the interface. A similar situation holds for low-energy electron diffraction[16] and scanning tunneling microscopy[14,15] experiments where the oxide is etched away and the roughness of the remaining Si surface is measured. These roughness parameters cannot be compared directly with our results. Vibrational spectroscopy[19] shows that the bonding changes when the oxide coverage is on the order of a monolayer. Oxygen is found to be incorporated into bridge bonds at elevated temperatures, as assumed in our models.

IX. SUMMARY

The aim of our work is to give a quantitative analysis of intermediate-oxidation states at the SiO_2/Si interface and to derive structural models from it. In order to achieve this we measure the escape depth in Si and SiO_2, and the photoionization cross section for various oxidation states of Si. From these calibration measurements the density of intermediate-oxidation states is determined. It corresponds to about two layers of Si atoms with a somewhat higher density for a Si(111) substrate than for Si(100). This high density and the observation of a strong Si^{3+} component rule out most of the existing interface models, which exhibit an atomically abrupt interface. Extended-interface models are given that are consistent with our results. They feature characteristic protrusions of Si^{3+} into the SiO_2 overlayer, which can be viewed as the cores of misfit dislocations. The extended interface structure appears to be strain driven, which is easy to understand given the large misfit in bond density between Si and SiO_2.

ACKNOWLEDGEMENTS

We acknowledge M. Liehr for providing calibrated oxide films and B. Robinson for ellipsometry measurements. Research was carried out in part at the National Synchrotron Light Source, Brookhaven National Laboratory, which is sponsored by the U.S. Department of Energy (Division of Materials Sciences and Division of Chemical Sciences of the Office of Basic Energy Sciences) under Contract No. DE-AC02-76CH0016.

---

*Present address: Surface Science Division, National Bureau of Standards, Gaithersburg, MD 20899.

[1] *The Physics of SiO_2 and its Interfaces,* edited by Sokrates T. Pantelides (Pergamon, New York, 1978).

[2] F. J. Grunthaner and P. J. Grunthaner, Mater. Sci. Rep. **1**, 65 (1986).

[3] See various articles in Philos. Mag. **55** (1987).

[4] Proceedings of the 173rd meeting of the Electrochemical Society, Atlanta, Georigia, 1988, edited by C. R. Helms (unpublished).

[5] F. Rochet, S. Rigo, M. Froment, C. D'Anterroches, C. Maillot, H. Roulet, and G. Dufour, Adv. Phys. **35**, 237 (1986).

[6] F. Herman, I. P. Batra, and R. V. Kasowski, in *The Physics of SiO_2 and its Interfaces,* Ref. 1, p. 333; F. Herman, and R. V. Kasowski, J. Vac. Sci. Technol. **19**, 395 (1981).

[7] S. T. Pantelides and Marshall Long, in *The Physics of SiO_2 and its Interfaces,* Ref. 1, p. 339.

[8] T. Hattori, M. Muto, and T. Suzuki, in *Proceedings of the 17th International Conference on the Physics of Semiconductors,* edited by D. J. Chadi and W. Harrison (Springer-Verlag, New York, 1985), p. 229.

[9] A. Ourmazd, D. W. Taylor, J. A. Rentschler, and J. Bevk, Phys. Rev. Lett. **59**, 213 (1987).

[10] I. Ohdomari, H. Akatsu, Y. Yamakoshi, and Koji Kishimoto, J. Non-Cryst. Solids **89**, 239 (1987).

[11] I. Ohdomari, H. Akatsu, Y. Yamakoshi, and K. Kishimoto, J. Appl. Phys. **62**, 3751 (1987).

[12] O. L. Krivanek and J. H. Mazur, Appl. Phys. Lett. **37**, 392 (1980).

[13] S. M. Goodnick, D. K. Ferry, C. W. Wilmsen, Z. Liliental, D. Fathy, and O. L. Krivanck, Phys. Rev. B **32**, 8171 (1985).

[14] A. H. Carim, M. M. Dovek, C. F. Quate, R. Sinclair, and C. Vorst, Science **237**, 630 (1987).

[15] W. J. Kaiser, L. D. Bell, M. H. Hecht, and F. J. Grunthaner, J. Vac. Sci. Technol. A **6**, 519 (1988).

[16] P. O. Hahn and M. Henzler, J. Vac. Sci. Technol. A **2**, 574 (1984); M. Henzler and P. Marienhoff, J. Vac. Sci. Technol B **2**, 346 (1984).

[17] B. Nielsen, K. G. Lynn, Y. C. Chen, and D. O. Welch, Appl. Phys. Lett. **51**, 1022 (1987).

[18] D. E. Aspnes and J. B. Theeten, J. Electrochem. Soc. **127**, 1359 (1980).

[19] H. Ibach, H. D. Bruchmann, and H. Wagner, Appl. Phys. A **29**, 113 (1982).

[20] M. Grundner and H. Jacob, Appl. Phys. A **39**, 73 (1986).

[21] R. Haight and L. C. Feldman, J. Appl. Phys. **53**, 4884 (1982).

[22] R. A. Cowley and T. W. Ryan, J. Phys. D **20**, 61 (1987); P. H. Fuoss, L. J. Norton, S. Brennan, and A. Fischer-Colbrie, Phys. Rev. Lett. **60**, 600 (1988).

[23] A. Cerezo, C. R. M. Grovenor, and G. D. W. Smith, J. Microsc. (Oxford) **141**, 155 (1986); C. R. M. Grovenor, A. Cerezo, and G. D. W. Smith, in *Layered Structures, Epitaxy, and Interfaces,* edited by J. M. Gibson and L. R. Dawson (MRS, Pittsburgh, 1985), p. 199; A. M. Stoneham, C. R. M. Grovenor, and A. Cerezo, in Ref. 3, p. 201.

[24] C. R. Helms, Y. E. Strausser, W. E. Spicer, Appl. Phys. Lett. **33**, 767 (1978); C. R. Helms, N. M. Johnson, S. A. Schwartz, and W. E. Spicer, J. Appl. Phys. **50**, 5007 (1979).

[25] J. Derrien and M. Commandré, Surf. Sci. **118**, 32 (1982).

[26] R. Flitsch and S. I. Raider, J. Vac. Sci. Technol. **12**, 305 (1975).

[27] F. J. Grunthaner, P. J. Grunthaner, R. P. Vasquez, B. F. Lewis, J. Maserjian, and A. Madhukar, Phys. Rev. Lett. **43**, 1683 (1979); J. Vac. Sci. Technol. **16**, 1443 (1979).

[28] M. H. Hecht, F. J. Grunthaner, P. Pianetta, L. I. Johanssonn, and I. Lindau, J. Vac. Sci. Technol. A **2**, 584 (1984).

[29] P. J. Grunthaner, M. H. Hecht, and F. J. Grunthaner, J. Appl. Phys. **61**, 629 (1987); M. H. Hecht, P. J. Grunthaner, and F. J. Grunthaner, in *Proceedings of the 17th International Conference on the Physics of Semiconductors,* edited by J. D. Chadi and W. A. Harrison (Springer-Verlag, New York, 1985), p. 217.

[30] J. M. Hill, D. G. Royce, C. S. Fadley, L. F. Wagner, and F. J. Grunthaner, Chem. Phys. Lett. **44**, 225 (1976).

[31] A. Ishizaka and S. Iwata, Appl. Phys. Lett. **36**, 71 (1980).

[32] T. Suzuki, M. Muto, M. Hara, T. Hattori, K. Yamabe, and H. Yamuauchi, in Proceedings of Extended Abstracts of the 16th International Conference on Soild State Devices and Materials, Kobe, 1984, p. 297 (unpublished).

[33] T. Hattori and T. Suzuki, Appl. Phys. Lett. **43**, 470 (1983); T. Hattori and T. Suzuki, in Proceedings of Extended Abstracts of the 16th International Conference on Solid State Devices and Materials, Ref. 32, p. 497.

[34] J. Finster, D. Schulze, F. Bechstedt, and A. Meisel, Surf. Sci. **151/153**, 1063 (1985).

[35] T. D. Bussing and P. H. Holloway, J. Vac. Sci. Technol. A **3**,

1973 (1985); T. D. Bussing, P. H. Holloway, Y. X. Wang, J. F. Moulder, and J. S. Hammond (unpublished).
[36]J. Halbritter, J. Mater. Reson. 3, 506 (1988).
[37]M. F. Hochella, Jr. and A. H. Carim, Surf. Sci. Lett. **197**, L260 (1988).
[38]C. M. Garner, I. Lindau, C. Y. Su, P. Pianetta, and W. E. Spicer, Phys. Rev. B **19**, 3944 (1979).
[39]M. Tabe, T. T. Chiang, I. Lindau, and W. E. Spicer, Phys. Rev. B **34**, 2706 (1986).
[40]A. Bianconi and R. S. Bauer, Surf. Sci. **99**, 76 (1980).
[41]G. Hollinger and F. J. Himpsel, J. Vac. Sci. Technol. A **1**, 640 (1983); Phys. Rev. B **28**, 3651 (1983).
[42]G. Hollinger and F. J. Himpsel, Appl. Phys. Lett. **44**, 93 (1984).
[43]W. Braun and H. Kuhlenbeck, Surf. Sci. **180**, 279 (1987).
[44]The pressure-versus-temperature equilibrium curve between a Si surface and O_2 (H_2O) is given in F. W. Smith and G. Ghidini, J. Electrochem. Soc. **129**, 1300 (1982); **131**, 2924 (1984).
[45]F. J. Himpsel, F. R. McFeely, J. F. Morar, A. Taleb-Ibrahimi, and J. A. Yarmoff, in *Proceedings of the 1988 Enrico Fermi School on Photoemission and Absorption Spectroscopy of Solids and Interfaces with Synchrotron Radiation, Varenna, 1988* (North-Holland, Amsterdam, in press).
[46]R. Tromp, G. W. Rubloff, P. Balk, F. K. Le Goues, and E. J. van Loenen, Phys. Rev. Lett. **55**, 2332 (1985).
[47]F. J. Himpsel, P. Heimann, T.-C. Chiang, and D. E. Eastman, Phys. Rev. Lett. **45**, 1112 (1980); F. J. Himpsel, D. E. Eastman, P. Heimann, B. Reihl, C. W. White, and D. M. Zehner, Phys. Rev. B **24**, 1120 (1981).
[48]For recent theoretical work on Si(100) see P. Krüger, A. Mazur, J. Pollmann, and G. Wolfgarten, Phys. Rev. Lett. **57**, 1468 (1986).
[49]The other half-layer of inner dimer atoms has opposite charge transfer and can be located about 0.2 eV below the bulk line by least-squares fitting. STM pictures of Si(100) show both symmetric and asymmetric dimers (Ref. 50). In our assignment the symmetric dimers are in fact rapidly oscillating asymmetric dimers. The time scale of the photoemission process is faster than the oscillation frequency, whereas the time scale of the STM experiment is slower. The surface core-level emission from Si has also been studied by D. H. Rich, T. Miller, and T.-C. Chiang, Phys. Rev. Lett. **60**, 357 (1987); Phys. Rev. B **37**, 3124 (1988). The surface core-level intensities (relative to the total intensity) obtained in this work [0.163 for Si(100) and 0.050 for Si(111) at $h\nu=150$ eV] are very similar to ours [0.17 for Si(100) and 0.05 for Si(111) at $h\nu=130$ eV]. However, a different assignment is given by Rich *et al.* which doubles the number of surface atoms corresponding to a given core-level intensity. Essentially, such an assignment is not compatible with the surface core-level intensities on other model surfaces [the As/Si(111)1×1 and CaF_2/Si(111)1×1 structures would give about two layers of Si with shifted core levels], and it is opposite to our knowledge about charge transfer at the Si(111)7×7 surface. Scanning tunneling spectroscopy (Ref. 50) and first-principles calculations (Ref. 51) find that electrons are transferred from adatoms to rest atoms to fill the dangling bond orbital of the rest atoms. Therefore, one would expect the rest atoms to exhibit the observed upwards core-level shift, and not the adatoms as in the assignment by Rich *et al.* Since there are about twice as many adatoms in the unit cell as rest atoms (12 vs 7) there is a factor of 2 discrepancy between the assignments.
[50]R. J. Hamers, R. M. Tromp, and J. E. Demuth, Phys. Rev. Lett. **56**, 1972 (1986); Surf. Sci. **181**, 346 (1987); Phys. Rev. B **34**, 5343 (1986).
[51]J. E. Northrup, Phys. Rev. Lett. **57**, 154 (1986).
[52]M. A. Olmstead, R. D. Bringans, R. I. G. Uhrberg, and R. Z. Bachrach, Phys. Rev. B **34**, 6401 (1986).
[53]F. J. Himpsel, F. U. Hillebrecht, G. Hughes, J. L. Jordan, U. O. Karlsson, F. R. McFeely, J. F. Morar, and D. Rieger, Appl. Phys. Lett. **48**, 596 (1986).
[54]D. Rieger, F. J. Himpsel, U. O. Karlsson, F. R. McFeely, J. F. Morar, and J. A. Yarmoff, Phys. Rev. B **34**, 7295 (1986); F. J. Himpsel, U. O. Karlsson, J. F. Morar, D. Rieger, and J. A. Yarmoff, Phys. Rev. Lett. **56**, 1497 (1986); Mater. Res. Soc. Symp. Proc. **94**, 181 (1987).
[55]M. A. Olmstead, R. I. G. Uhrberg, R. D. Bringans, and R. Z. Bachrach, Phys. Rev. B **35**, 7526 (1987).
[56]S. Tanuma, C. J. Powell, and D. R. Penn (unpublished).
[57]F. R. McFeely *et al.* (unpublished).
[58]D. Schmeisser, F. J. Himpsel, and G. Hollinger, Phys. Rev. B **27**, 7813 (1983).
[59]H. Ibach, W. Wagner, and D. Bruchmann, Solid State Commun. **42**, 457 (1982); E. M. Oellig, R. Butz, H. Wagner, and H. Ibach *ibid.* **51**, 7 (1984); Y. Chabal, Phys. Rev. B **29**, 3677 (1984).
[60]The surface to bulk+surface intensity ratio is 1.01 times greater for Si(111) terminated by a single dangling bond than for Si(100) at $h\nu=130$ eV, see Eqs. (4), (5a), and (5b), and Table I.
[61]N. M. Johnson, D. K. Biegelsen, M. D. Moyer, and S. T. Chang, Appl. Phys. Lett. **43**, 563 (1983). The distribution of P_b centers is given for the SiO_2/Si(111) interface, but a similar distribution is expected on Si(100).
[62]A. H. Edwards, Phys. Rev. B **36**, 9638 (1987).
[63]F. K. Le Goues *et al.* (unpublished).
[64]K. Siegbahn, Philos. Trans. R. Soc. London **A318**, 3 (1986).
[65]L. Pauling, *The Nature of the Chemical Bond* (Cornell University Press, Ithaca, New York, 1948).
[66]E. Yablonovitch, D. L. Allara, C. C. Chang, T. Gmitter, and T. B. Bright, Phys. Rev. Lett. **57**, 149 (1986).
[67]B. S. Meyerson, F. J. Himpsel, and J. A. Yarmoff (unpublished).
[68]J. F. Morar and J. Bevk (unpublished).
[69]G. Hughes, G. Hollinger, J. F. Morar, and F. J. Himpsel (unpublished).
[70]The Si(100) surface terminated by (111) facets can exhibit Si^{3+} at the expense of creating a higher bond density at the Si surface. We can rule out such a model by observing that the distribution of intermediate-oxidation states for Si(100) differs from that for Si(111).
[71]F. J. Himpsel, G. Hollinger, and R. A. Pollak, Phys. Rev. B **28**, 7014 (1983).
[72]Z. A. Weinberg, G. W. Rubloff, and E. Bassous, Phys. Rev. B **19**, 3107 (1979). A somewhat larger band gap of 9.7 eV has been reported for SiO_2 by V. J. Nithianandam and S. E. Schnatterly (unpublished).
[73]Z. A. Weinberg and A. Hartstein, J. Appl. Phys. **54**, 2517 (1983).
[74]G. Hollinger, R. Saoudi, P. Ferret, M. Pitaval, in Proceedings of the 173rd meeting of the Electrochemical Society, Atlanta, Georgia, 1988 (unpublished).